# Collective behavior of laser-produced plasma from a multicomponent $YBa_2Cu_3O_7$ target in air

**R.C. Issac, G.K. Varier, S.S. Harilal, V.P.N. Nampoori, C.P.G. Vallabhan**

Laser Division, International School of Photonics, Cochin University of Science & Technology, Cochin 682 022, India

**Abstract.** The dynamics of diffusion of electrons and ions from the laser-produced plasma from a multielement superconducting material, namely $YBa_2Cu_3O_7$, using a Q-switched Nd:YAG laser is investigated by time-resolved emission-spectroscopic techniques at various laser irradiances. It is observed that beyond a laser irradiance of $2.6 \times 10^{11}$ W cm$^{-2}$, the ejected plume collectively drifts away from the target with a sharp increase in velocity to $1.25 \times 10^6$ cm s$^{-1}$, which is twice its velocity observed at lower laser irradiances. This sudden drift apparently occurs as a result of the formation of a charged double layer at the external plume boundary. This diffusion is collective, that is, the electrons and ions inside the plume diffuse together simultaneously and hence it is similar to the ambipolar diffusion of charged particles in a discharge plasma.

Laser-produced plasmas, obtained when high-power laser beams interact with solids, have evoked a great deal of attention both in basic and applied fields of research [1–7]. The study of the transport properties in laser-produced plasmas can shed light on the different mechanisms involved in their formation and evolution in time and space. Laser plasmas generated in low ambient gas pressures have a wide range of applications as in materials analysis [8] and thin-film deposition of materials such as metals, ferroelectrics, semiconductors, and high-$T_c$ superconductors [9–16]. Recently fabrication of stoichiometric films of high-$T_c$ superconductors in air at atmospheric pressure have been reported [17, 18]. Plasmas formed at atmospheric pressure have a high temperature and density, and the concentrations of the various species may become close to the stoichiometric proportions in the target. With $YBa_2Cu_3O_7$ as target, laser plasmas formed at atmospheric pressure exhibit time-dependent emission characteristics and opacity [19]. Resonance lines are found to be severely self-reversed and they show anomalous line profiles due to anisotropic resonance scattering [20].

Laser–target interaction leads to rapid expansion and the velocities of ejected species generally depend on their masses, which vary for of atoms, molecules, or clusters. A slight deviation from charge neutrality at the external plume boundary may create large electric fields because of the formation of a charged double layer, which results in the acceleration of individual charged particles [21–24]. Such charged double layers can be formed in laser-produced plasmas with electron densities in the range $10^6$–$10^{21}$ cm$^{-3}$ [21]. Double layers play a very important role in different contexts ranging from astrophysical processes to plasma confinement in fusion devices [25]. Here we report the collective diffusion of ions and electrons in the plasma plume as a whole due to the electric fields created by charged double layers of electrons and ions.

## 1 Experimental details

The schematic of the basic experimental setup for the present study is given in Fig. 1. High-power laser radiation from a Q-switched Nd:YAG (Quanta Ray DCR 11) laser at wavelength $1.06\,\mu m$ with pulse duration 10 ns is focused (estimated focal-spot radius $50\,\mu m$ at the target) to produce the plasma in air ambient at atmospheric pressure. The target used in our studies was a disk of $YBa_2Cu_3O_7$ of radius 1.75 cm and thickness 0.5 cm that was mounted axially on the shaft of a dc motor and was rotated about the axis in order to avoid multiple hits at the same spot for a long time, which would result in the pitting of the target. The optical emission from the plasma at various spatial positions (with spatial resolution better than 0.3 mm) away from the target surface was monitored after one-to-one imaging of the plasma segments on to the entrance slit of a monochromator by appropriate collimating or focusing lenses and by apertures. The spectrometer used was a 1-m monochromator (SPEX model 1740, grating with 1200 grooves per mm blazed at 500 nm and having a slit-width-limited resolution of 0.015 nm). A thermoelectrically cooled photomultiplier tube (Thorn EMI) was used as the light sensor. The time evolution of the emission spectrum at a par-
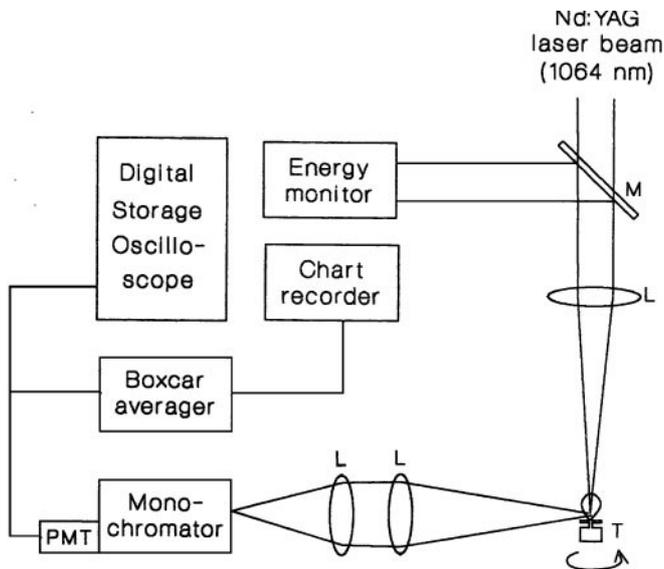
**Fig. 1.** Schematic of the experimental setup: M – 10% reflector; L – lenses; T – rotating target; P M T – photomultiplier tube



**Fig. 2.** The emission spectrum at two different laser irradiances at a distance 0.5 mm from the target; (a) $1.9 \times 10^{11}$ W cm$^{-2}$ (b) $3 \times 10^{11}$ W cm$^{-2}$. The *curves* are identical except for a threefold decrease in intensity at higher laser irradiance. The intensities are peak values of the time-dependent signal recorded after averaging intensities from ten pulses and maximum error in intensity measurements is 5%

ticular distance from the target was monitored on a 200-MHz digital storage oscilloscope (DS 8621, IWATSU). The spectral recording was done on a chart recorder after averaging intensities from 10 successive pulses using a boxcar averager (Stanford Research Systems, SRS 250). The laser pulse energy was measured using a calibrated laser energy meter and the irradiance at the focal spot was calculated after making reflection corrections from lens surfaces.

## 2 Results and discussion

Laser-produced plasmas at atmospheric pressure are dense and confined to small volumes due to the inward force exerted by the atmospheric gases. The apparent length of the light-emitting zone in the plume was about 5 mm in the present case. Interferometric measurements [19] on YBa$_2$Cu$_3$O$_7$ plasma in air show that plasma electron density was of the order of $10^{16}$–$10^{17}$ cm$^{-3}$. It was also found that at high laser irradiances, the main ionization mechanism in the plasma is collision dominated whereas at relatively low laser irradiances multiphoton processes take place [19]. The high density and collision rate inside the plasma favors the existence of local thermodynamic equilibrium [28]. The diffusion characteristics of the plasma are found to vary significantly with laser irradiance on the target. Plasma emission very close to the target is monitored using the setup mentioned above and the optical emission spectrum at a laser irradiance of $1.9 \times 10^{11}$ W cm$^{-2}$ is recorded in the region 350 nm to 650 nm (Fig. 2a). The spectrum shows mostly ionic emission lines from different constituents inside the plasma together with a few atomic lines. Less intense lines from singly and doubly ionized nitrogen present in air also are observed in a more resolved spectra. Figure 2b represents the spectrum at $3 \times 10^{11}$ W cm$^{-2}$, which shows a threefold decrease in emission intensity for all the lines. This apparently anomalous behavior at higher laser irradiances is explained later in the text. In order to estimate the plasma expansion time, the monochromator was set at 500 nm where there is con-
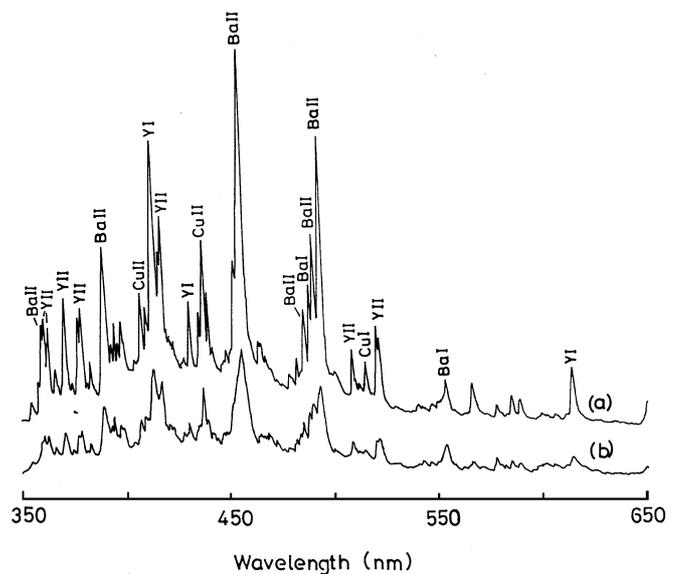
tinuum with no line emissions and the expansion time and emission intensity were measured from the oscilloscope display. The main reason for selecting plasma continuum for this study is that the positive ions and electrons are responsible for the blackbody continuum since plasma continuum essentially originates from the bremsstrahlung radiation and radiative recombination [28].

Measurements on the plasma expansion time at various laser irradiances were carried out. Figure 3 shows a plot of the laser irradiance vs. the plasma expansion time at a distance 0.5 mm from the target surface. At very low laser irradiances, there is a sudden decrease in the plasma expansion time as
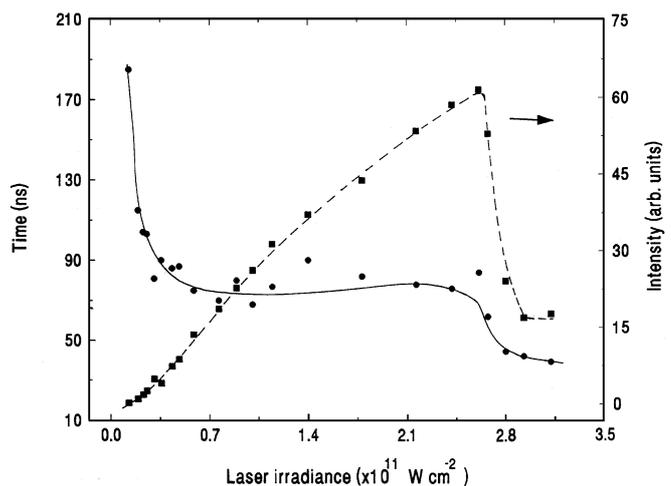


**Fig. 3.** Variation of plasma expansion time (●) and continuum intensity (■) as a function of laser power density. At a laser irradiance of $\approx 2.6 \times 10^{11}$ W cm$^{-2}$, the expansion time decreases to about half the initial value. Exactly at this point the continuum emission intensity also decreases sharply. Measurement conditions are the same as those for Fig. 2

the laser irradiance is slowly increased. On further increase of the laser irradiance, the expansion time remains at a steady value of about 83 ns. This initial sharp increase in the velocity at low irradiances is due to the plasma expansion resulting from the very high internal pressure developed at the ablation spot where the ejected material acts as a piston that drives a spherical blast wave into the ambient gas. But this pressure reaches a steady state and consequently the expansion velocity assumes a constant value of $6.02 \times 10^5 \, \text{cm s}^{-1}$. This happens when the laser light is screened, in the sense of not being absorbed by the target, due to reflection by the high density plasma at the critical density surface. But when the laser irradiance is increased further, to $\approx 2.6 \times 10^{11} \, \text{W cm}^{-2}$, the expansion time suddenly decreases to approximately half the initial value, namely, 40 ns with a fourfold increase in the kinetic energy. This means that the expansion velocity of the plasma has suddenly doubled at this laser irradiance to a typical value of $1.25 \times 10^6 \, \text{cm s}^{-1}$. It is also apparent from Fig. 3 that the intensity of plasma continuum emission falls steeply at this laser irradiance. Ionic and atomic line emissions also suffer reduction in intensity as can be seen from Fig. 2b, which is the optical emission spectrum from the plasma at a laser irradiance of $3 \times 10^{11} \, \text{W cm}^{-2}$. The spectrum is similar to that obtained at $1.9 \times 10^{11} \, \text{W cm}^{-2}$ (Fig. 2a) but with reduction in emission intensity for all the lines. This is due to a reduction in particle density integrated along the line of sight near the target surface, i.e. the plasma as a whole drifts away from the target thereby producing a rarefaction near the target. Thus at higher laser irradiances two distinct types of plasma motion occur, the radial expansion as well as the sudden drift of the plasma as a whole normal to the target. The radial expansion becomes dominant only after the plasma has drifted to a certain distance away from the target surface, which in turn depends on the value of laser irradiance.

Figure 2a shows the spectrum at a laser irradiance of $1.9 \times 10^{11} \, \text{W cm}^{-2}$, which exhibits emission lines from all atomic and ionic species when only hydrodynamic radial expansion is predominant. However in Fig. 2b the intensities of all these lines have gone down by a factor of nearly three. This means that the number densities of almost all the species with different ionization states integrated along the line of sight are low near the surface for laser irradiances above $2.6 \times 10^{11} \, \text{W cm}^{-2}$, indicating the collective nature of the expansion process. This holds good for a range of laser irradiances above the threshold of $2.6 \times 10^{11} \, \text{W cm}^{-2}$. At these irradiances, when observed normal to the plasma expansion direction (expansion direction is always normal to the target surface), the section with maximum intensity of plasma emission is at a region farther away from the target surface. The spectra recorded at the maximum intensity region is the same as the one close to the target at low laser irradiance but with slightly reduced line widths.

The irradiation of a target with very high intensity lasers produce temperatures well above the thermodynamic critical temperature and the main mechanism of ablation is 'phase explosion' rather than 'vapourization' [26, 27]. Radial expansion takes place because of the very high pressure developed following ablation of the target material leading to velocities of the order of $10^5 \, \text{cm s}^{-1}$ for the plume expansion front. There exists a steep density gradient along the radial direction in a laser-produced plasma. The density of electrons has a larger value towards the target surface and at some point

nearer to the target the density exceeds the critical density which is defined as

$$n_{ec} = \frac{\omega^2 m_e \epsilon_0}{e^2}, \tag{1}$$

where $\omega = 2\pi\nu$, $\nu$ is the frequency of laser light, $m_e$ is the mass of electron, $e$ is the electron charge and $\epsilon_0$, the permitivity of free space. The laser beam penetrates into the plasma only if the density is less than the critical density. Therefore the laser-ablated plume consists of two regions, the outer corona ($n_e \leq n_{ec}$), and the conduction region ($n_e > n_{ec}$). A surface which separates the two is called the critical density surface. (One should not expect a sharp boundary between the conduction region and the outer corona and the critical density surface may not be thought of as infinitely thin). In the outer corona of the plume where the electron density is less than the critical density, the laser energy is absorbed by the electrons directly. The attenuation of the laser light as it traverses the plume is given by [21]

$$I_a = I_0 \left[ 1 - \exp\left( -\frac{32}{15} k_{IB} L \frac{\nu_c}{\omega} \right) \right], \tag{2}$$

where $I_0$ and $I_a$ are the incident and the absorbed laser intensities for electron density $n_e$ less than the critical density $n_{ec}$, $k_{IB}$ is the inverse bremsstrahlung absorption coefficient, $\nu_c$ is the collision frequency which goes down with temperature as $\nu_c \approx T_e^{-3/2}$. The scale length $L$ is the distance over which the electron density changes from zero to $n_{ec}$. The energy absorbed by the corona electrons is transferred to the conduction region. If the heating rate of the corona electrons is much larger than the losses to the conduction region, the temperature of the corona electrons will rise and a temperature gradient may be formed. Therefore we can write [29]

$$\frac{dT_e}{dx} \geq \frac{T_e}{\lambda_{ee}}, \tag{3}$$

where $\lambda_{ee}$ is the mean free path for e–e collisions. The temperature gradient may be accompanied by an electric field given by

$$E \approx \frac{k}{e} \frac{dT_e}{dx} \tag{4}$$

and some of the electrons may be accelerated out of the corona [29]. The loss of hot electrons creates a large potential, which limits the total number of electrons that can be thrown off [19, 30]. The electron heating will cease when the laser pulse is terminated. Thus ions inside the plume can be accelerated in the electric field generated by the fast electrons escaping from the plume.

Normally the diffusion coefficients of electrons ($D_e$) and ions ($D_i$) are different with their ratio given by [32], $(D_e/D_i) \propto (v_e/v_i) \propto (M/m)^{1/2}$, and it is clear that the relative values obey $D_e \gg D_i$. The fast escaping electrons produce a region in which there is a separation between the ion and electron clouds. These positive and negative charge clouds are in most cases separated by a characteristic distance that is of the order of the Debye length [21]. But in the case of a deviation from charge neutrality the ions are accelerated in the electric field produced by the fast electrons receding

from the plume and the plume as a whole begins to propagate with twice the diffusion coefficient of the ions similar to that in a discharge plasma [32].

Since the ions have a velocity less than that of the electrons, the fast electrons will create a situation in which the positive and negative charges are well separated. The electric field thus generated may be represented in terms of the electron velocity and density given by [23]

$$E = -\frac{m_e v_e^2}{e} \frac{\partial(\ln N_e)}{\partial z} , \qquad (5)$$

where $m_e$ and $v_e$ are the electron mass and velocity respectively, $e$ the electron charge, and $N_e$ the electron density in the plume. In the present experiment, the propagation direction of the plasma coincides with the $z$ axis which is normal to the target. One can make a rough estimate of the electric field by considering the additional velocity of the ions $v_i$, to be solely due to the electric field created by the separated electrons and ions after introducing a characteristic ion velocity [23] $v_i^2 = (2Z_i m_e v_e^2)/M_i$ ($v_i = 1.25 \times 10^6$ cm s$^{-1}$ in the present case), where $M_i$ is the average mass of the ions and $Z_i$ their average charge. Then, with $Z_i = 1$, average mass number 45, $\Delta z \approx 0.05$ μm, (the typical length over which the field is applicable, i.e., the Debye length for an electron density $10^{17}$ cm$^{-3}$ and electron temperature 5 eV), $\Delta N_e/N_e = 0.01$, and $E \approx 1.4 \times 10^5$ V cm$^{-1}$. That is, a 1% change in the electron density over a distance of the order of the Debye length produces electric fields of the order of $10^5$ V cm$^{-1}$.

The collective nature of the expansion process shows that it is similar to ambipolar diffusion in a discharge plasma. The differential equation which governs the diffusion process becomes [32]

$$\frac{\partial N_i}{\partial t} = 2D_i \Delta N_i . \qquad (6)$$

Here $N_i$ is the ion number density and $\Delta N_i$ refers to the change in ion number density over a distance equal to the Debye length. This is the equation governing the diffusion of ions with $D_i$ replaced by $2D_i$ resulting from the coupling of diffusion processes of electrons and ions, and mutual interaction of the electron and ion clouds. The electrons and ions diffuse together with twice the diffusion coefficient of the ions when there is a deviation from the total charge neutrality. Since the diffusion coefficient is directly proportional to the velocity, the observed increase in the velocity to approximately double the initial velocity takes place. The collective nature of the diffusion process shows that the drift mechanism is similar to ambipolar diffusion.

The continuum emission intensity is maximum near the target surface and decreases with increasing separation from the target. Figure 4 shows a plot of emission intensity vs. the laser irradiance at three different distances from the target surface, namely, 0.05 cm, 0.2 cm, and 0.4 cm. At laser irradiances greater than $2.6 \times 10^{11}$ W cm$^{-2}$ the plasma continues to move with the same velocity but the plume as a whole is shifted to greater distances. These results show that at a distance 0.2 cm away from the target the emission peaks at a laser irradiance of $2.84 \times 10^{11}$ W cm$^{-2}$, whereas at 0.4 cm the emission maximizes at a laser irradiance of $3.05 \times 10^{11}$ W cm$^{-2}$. It is evident from these observations that
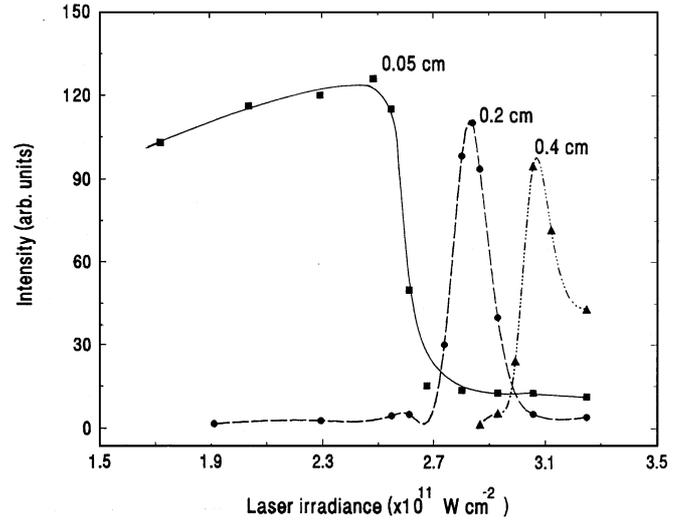


**Fig. 4.** Variation of continuum emission intensity at 500 nm at three different distances from the target. Measurement conditions are the same as those for Fig. 2

the plasma plume has drifted farther and farther away from the target as the input laser irradiance is increased.

## 3 Conclusions

We have described some aspects of the diffusion dynamics of laser-produced plasma from the multielement superconductor YBa$_2$Cu$_3$O$_7$ using time-resolved spectroscopy at laser irradiance levels ranging from $2.5 \times 10^9$ W cm$^{-2}$ to $3.5 \times 10^{11}$ W cm$^{-2}$. At low laser irradiances only radial expansion occurs, whereas beyond a threshold of $2.6 \times 10^{11}$ W cm$^{-2}$ the plasma as a whole drifts collectively away from the target surface in the electric field produced by the formation of a charged double layer at the external plume boundary. A rough estimate shows that an electric field of the order of $10^5$ V cm$^{-1}$ is generated at the plume expansion front. The collective nature of the diffusion is similar to ambipolar diffusion in a discharge plasma and it ensures that the stoichiometry of the various atoms and ions in the plume near the target surface is preserved at a farther distance from the target. As the input laser irradiance is increased the plume propagates to farther distances in air within a nanosecond time scale. In short, this paper demonstrates the formation of a charged double layer in air at atmospheric pressure and its role in the dynamics of ablation products.

## References

1. P. Engst, P. Kubat, P. Bohacek, J. Wild: Appl. Phys. Lett. **64**, 2025 (1994)
2. R. Kelly, A. Miotello: Appl. Phys. B **57**, 145 (1993)
3. D.B. Geohegan: Thin Solid Films **220**, 138 (1992)
4. R.E. Russo: Appl. Spectrosc. **49**, 14A (1995)
5. J. Gonzalo, C.N. Afonso, I. Madariaga: J. Appl. Phys. **81**, 951 (1997)

6. K.L. Saegner: Proc. Adv. Mater. **2**, 1 (1993); ibid **3**, 63 (1993)
7. S.S. Harilal, R.C. Issac, C.V. Bindhu, V.P.N. Nampoori, C.P.G. Vallabhan: J. Appl. Phys. **81**, 3637 (1997)
8. A. Ganzalea, M. Ortiz, J. Campose: Appl. Spectrosc. **49**, 1632 (1995)
9. D.B. Chrisey, G.K. Hubler (Eds.): *Pulsed Laser Deposition of Thin Films* (Wiley, New York 1994)
10. C. Champeaux, P. Marchet, J. Aubreton, J.P. Mercurio, A. Catherinot: Appl. Surf. Sci. **69**, 335 (1993)
11. R.K. Singh, J. Narayan: Phys. Rev. B **41**, 8843 (1990)
12. D.S. Misra, S.B. Palmer: J. Appl. Phys. **68**, 1403 (1990)
13. H. Jiang, A.J. Drehman, R.J. Andrews, J.A. Horrigan: Appl. Phys. Lett. **65**, 3132 (1994)
14. Y. Nakata, T. Okada, M. Maeda: Jpn. J. Appl. Phys. **34**, 4079 (1995)
15. P. Tiwari, S. Sharan, J. Narayan: Appl. Phys. Lett. **59**, 357 (1991)
16. T. Venkatesan, X.D. Wu, B. Dutta, A. Inam, M.S. Hegde, D.M. Hwang, C. Chang, L. Nazar, B. Wilkens: Appl. Phys. Lett. **54**, 581 (1989)
17. J. Wild, P. Engst, S. Civis, J. Pochyly: Appl. Phys. Lett. **60**, 1747 (1992)
18. J. Wild, P. Bohacek, J. Macl, P. Engst, J. Pracharova, J. Pochyly: Physica C **209**, 486 (1993)
19. G.K. Varier, R.C. Issac, S.S. Harilal, C.V. Bindhu, V.P.N. Nampoori, C.P.G. Vallabhan: Spectrochim. Acta B **52**, 657 (1997)
20. R.C. Issac, S.S. Harilal, G.K. Varier, C.V. Bindhu, V.P.N. Nampoori, C.P.G. Vallabhan: Spectrochim. Acta B **52**, 1791 (1997)
21. S. Eliezer, H. Hora: Phys. Rep. **172**, 339 (1989)
22. S. Eliezer, H. Hora, E. Kolka, F. Green, H. Szichman: Laser Part. Beams **13**, 441 (1995)
23. E.G. Gamaly: Phys. Fluids B **5**, 944 (1993)
24. E.G. Gamaly: Laser Part. Beams **12**, 185 (1994)
25. See for example references cited in [21]
26. R. Kelly, M. Miotello: Appl. Surf. Sci. **96**–**98**, 205 (1996)
27. R. Kelly, M. Miotello: Nucl. Instrum. Methods Phys. Res., Sect. B **122**, 374 (1997)
28. H.R. Griem: *Plasma Spectroscopy* (McGraw-Hill, New York 1964)
29. T.P. Hughes: *Plasmas and Laser Light* (Adam Hilger, Bristol 1975) p. 329
30. R.D. Brooks, R.G. Benzer, Z.A. Pietrzyk: In *Laser Interaction and Related Plasma Phenomena*, Vol. 6, ed. by H. Hora, G.H. Miley (Plenum, New York 1984) p. 479
31. R.E. Russo: Appl. Spectrosc. **49**, 14A (1995)
32. E.M. Lifshitz, L.P. Pitaevskii: *Physical Kinetics* (Pergamon, New York 1981) p. 108